FOXM1 downregulation is a trigger of isatuximab-induced direct cell death in multiple myeloma cells with 1q+

Targeted therapies like proteasome inhibitors (PI), immunomodulatory drugs (IMiD), and/or anti-CD38 antibody have significantly improved the prognosis of patients with multiple myeloma (MM).[1,2] However, the prognoses with high-risk chromosome abnormalities (CA), such as t(4;14), t(14;16), del(17p), and gain/amplification of 1q (designated as 1q+), remain poor.[3] The anti-CD38 antibody, isatuximab (Isa), can significantly prolong the progression-free survival of relapsed and refractory MM (RRMM) patients carrying 1q+.[4] However, daratumumab, another anti-CD38 antibody, has been largely ineffective.[5] While both antibodies confer antibody-dependent immune effector cell-mediated cytotoxicity, Isa can directly induce the death of MM cells even in the absence of immune effector cells.[6] This led us to hypothesize that direct cell death may provide clinical benefit to MM patients with 1q+.

A previous study has shown that the transcription factor *PBX1*, which is located in the 1q23 region, is strongly associated with poor prognosis of MM patients with 1q+. *PBX1* is overexpressed in 1q+ MM cells and confers drug resistance by transactivating the downstream target genes including *E2F1/E2F2*, *FOXM1*, and *NEK2*.[7] We found significant upregulation of these factors in 1q+ MM cells, and high expression levels of *FOXM1*, *E2F2*, or *MCL1* were associated with worse prognosis in 1q+ MM patients after total therapy 2 and 3 (TT2/3) (*Online Supplementary Figure S1A*). In addition, FOXM1 was essentially found to be expressed only in the 1q+ MM cell lines compared to the cells with a normal copy number of 1q (designated as $1q^{normal}$ throughout the manuscript). In contrast, E2F2 showed a variable expression pattern among the 1q+ MM cell lines, while MCL1 was expressed in all cell lines regardless of 1q copy number (Figure 1A; *Online Supplementary Figure S1B*). Furthermore, both genetic knockdown and pharmacological inhibition of FOXM1 significantly inhibited the growth of 1q+ MM cell lines but did not have any impact on the $1q^{normal}$ cell lines (*Online Supplementary Figure S1C*). These results suggest an indispensable role of FOXM1 in the growth and survival of 1q+ MM cells.

There is evidence that Isa can directly induce death of CD38-overexpressing MM cells.[8,9] To this end, we overexpressed the *CD38* gene in the KMM.1 and KMS28-BM sublines that respectively harbor six copies of 1q (1q amp) and three copies of 1q (1q gain) with t(4;14). As expected, Isa significantly inhibited the growth of both sublines even in cells with high-risk CA, along with marked incorporation of Isa into MM cells. However, other antibodies, Elo-m and Dara-m, did not have any impact on the sublines (Figure 1B). We also determined the effect of these antibodies on the expression of FOXM1, E2F2, and MCL1 in the two sublines. Of these, we found that Isa downregulated FOXM1 protein expression in both sublines (Figure 1B; *Online Supplementary Figure S1D*). Consistent with these results, Isa downregulated FOXM1 in primary MM cells derived from patients with 1q+, but not in the $1q^{normal}$ cells (*Online Supplementary Figure S1E*). Informed consent was obtained in accordance with the Declaration of Helsinki, and the protocol was approved by the Institutional Review Board of Jichi Medical University. On the other hand, no significant changes were detected in the expression of E2F2 and MCL1 in either subline (Figure 1B; *Online Supplementary Figure S1D*). In addition, Elo-m and Dara-m had no significant effect in their expression levels (Figure 1B). A previous study had shown that the uptake of large amounts of monoclonal antibodies into the cells led to the enlargement and degradation of lysosomes, and the subsequent degradation of intracellular proteins by lysosomal proteases like cathepsins triggered non-apoptotic lysosomal cell death (LCD). In addition, concanamycin A (Con-A), an inhibitor of vacuolar ATPases, suppressed LCD by blocking antibody-induced lysosomal enlargement and degradation.[8] Consistent with the results, we found that Con-A mitigated Isa-induced growth inhibition, which coincided with restored FOXM1 expression (Figure 1C). These results suggest that FOXM1 protein is likely degraded by the lysosomal proteases. In contrast, daratumumab was not sufficiently incorporated into the MM cells to induce FOXM1 protein degradation by lysosomal proteases (Figure 1B).

To further validate the mechanism underlying Isa-induced growth inhibition, we established two FOXM1-overexpressing MM cell lines. As expected, forced expression of FOXM1 significantly mitigated the inhibitory effects of Isa in both sublines (Figure 1D). In contrast, FOXM1 knockdown augmented Isa-induced growth inhibition (*Online Supplementary Figure S1F*). Given that reactive oxygen species (ROS) mediate antibody-induced direct cell death,[9] and FOXM1 inhibitors can trigger ROS production in cancer cells,[10,11] we also measured the intracellular ROS levels. Consistent with the results, the FOXM1 inhibitor thiostrepton significantly inhibited the growth of MM cells by enhancing ROS production (*Online Supplementary Figure S1G*). In addition, forced expression of FOXM1 significantly suppressed ROS production (Figure 1D). These results suggest that Isa downregulates FOXM1 protein by lysosomal protease-mediated degradation, resulting in direct cell death through ROS production in 1q+ MM cells.

Recent clinical trials have shown that Isa in combination with pomalidomide (Poma) or carfilzomib (CFZ) prolonged the survival of RRMM patients with 1q+.[4] Previous studies

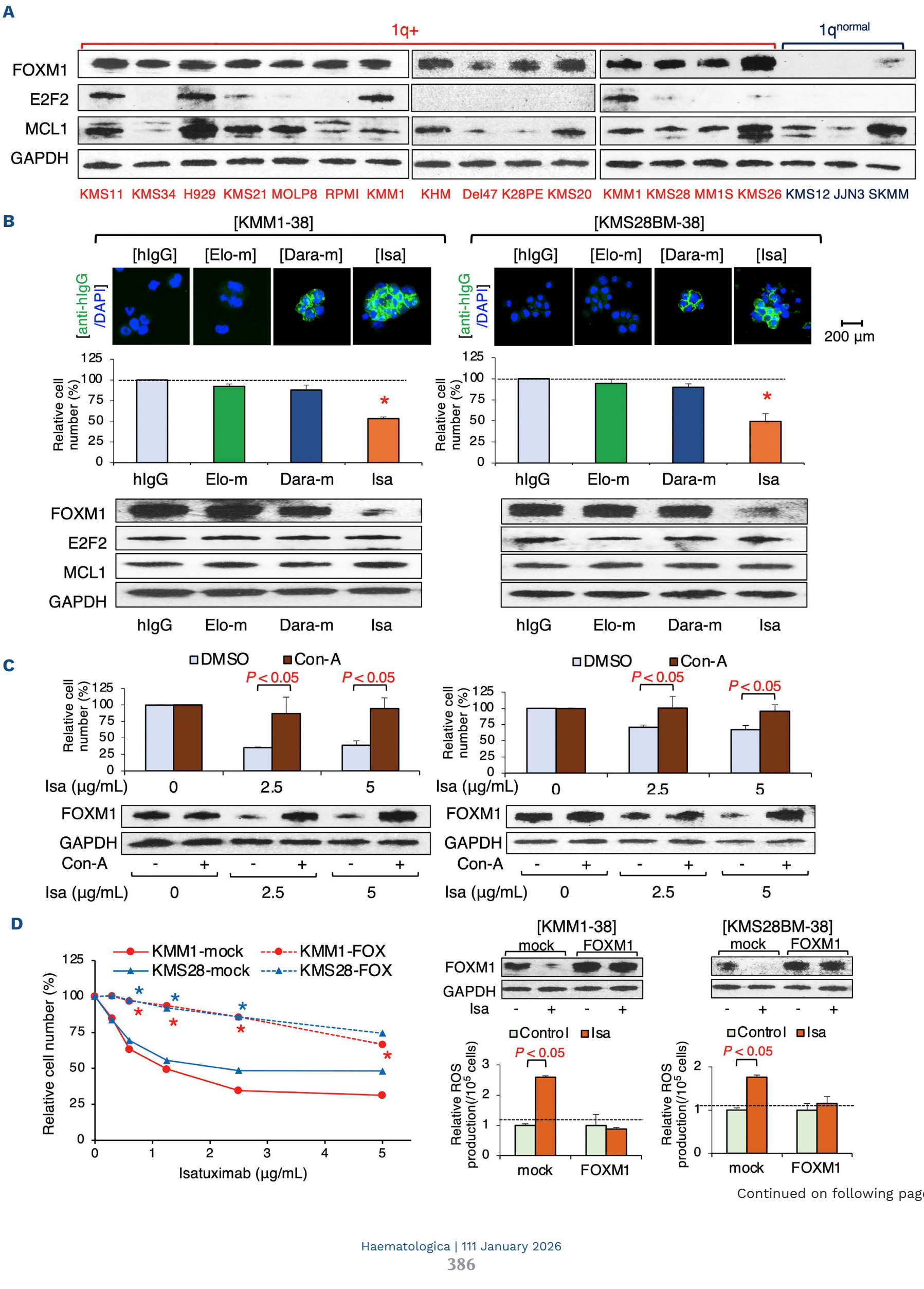

Continued on following page.

Figure 1. Isatuximab downregulates FOXM1 protein and induces reactive oxygen species-mediated direct cell death in 1q+ multiple myeloma cells. (A) Whole cell lysates were prepared from 1q+ and $1q^{normal}$ multiple myeloma (MM) cell lines and subjected to immunoblot for FOXM1, E2F2, and MCL1 using GAPDH as the loading control. Immunoblotting was carried out according to a standard method using the following antibodies: anti-FOXM1 (#20459), anti-MCL1 (#4572) (Cell Signaling Technology [CST], MA, USA); anti-E2F2 (sc-9967), and anti-GAPDH (Santa Cruz Biotechnology, CA, USA). The copy number of chromosome 1q was detected by fluorescence *in situ* hybridization (FISH) using the *CKS1B* FISH probe; 1q gain was defined as having 3 copies of *CKS1B*, and 1q amp was defined as having ≥4 copies of *CKS1B*. MM cell lines KMS12BM, JJN3, and SKMM1 with 2 copies of chromosome 1q (normal), KMS26, KMS28-BM, KMS-28PE (K28PE), KMS34, KMS11, RPMI8226, MM1.S, KMS21, NCI-H929, and MOLP8 with 3 copies of chromosome 1q (1q gain), and KMM.1, KHM1B (KHM), Delta47 (Del47), and KMS20 with 4< copies of chromosome 1q (1q amp) were procured from Health Science Research Resources Bank. In addition, KMS12BM, SKMM1, and MOLP8 harbor t(11;14). KMS26, KMS28-BM, KMS28-PE, KMS34, KMS11, and NCI-H929 harbor t(4;14). The FISH analyses were outsourced to SRL Inc. (Tokyo, Japan). (B) CD38-overexpressing KMM.1 and KMS28-BM sublines were established (denoted as KMM.1-38 and KMS28BM-38 respectively), and cultured in the presence of 5 μg/mL human immunoglobulin (hIgG), elotuzumab-mimic (Elo-m), daratumumab-mimic (Dara-m), and isatuximab (Isa) for 24 h. We used the lentiviral vector CSII-CMV-MCS-IRES-VENUS (provided by Dr. Hiroyuki Miyoshi, RIKEN BioResource Center, Ibaraki, Japan) containing the coding regions of *CD38* cDNA. Upper panel: cytospin specimens were prepared and stained with FITC-conjugated anti-hIgG antibody (green). Nuclei were counterstained with DAPI (blue). Only merged images are shown. Middle panel: cell proliferation was assessed by the MTT reduction assay using the Cell Counting Kit (Wako Biochemicals, Osaka, Japan). Data is shown relative to that of the corresponding hIgG controls. Data are the means ± standard deviation (S.D.) (bars) of multiple independent experiments (N=3); **P*<0.05 compared to the corresponding hIgG control was determined by one-way ANOVA with Student-Newman-Keuls multiple comparison test. The KaleidaGraph software (Synergy Software, Reading, PA, USA) was used for all statistical analyses. *P* values less than 0.05 were considered significant. Lower panel: immunoblot showing the expression of FOXM1, E2F2, MCL1, and GAPDH (loading control). (C) KMM.1-38 and KMS28BM-38 cells were cultured in the presence of Isa at the indicated concentrations with or without 1 nM concanamycin A (Con-A) for 24 hours (h). Upper panel: cell proliferation was assessed by the MTT reduction assay and the data is shown relative to that of the corresponding untreated controls. Data are the means ± S.D. (bars) of multiple independent experiments (N=3); *P* values were determined by one-way ANOVA with a Student-Newman-Keuls multiple comparison test. Lower panel: immunoblot showing the expression of FOXM1 and GAPDH (loading control). (D) KMM.1-38 and KMS28BM-38 cells were transduced with *FOXM1*-expressing (FOX) or empty (mock) lentiviral vector, and the stable transformants were cultured with different concentrations of isatuximab (Isa) for 24 h. We used the lentiviral vector CSII-CMV-MCS-IRES-VENUS containing the coding regions of *FOXM1* cDNA for gain-of-function experiments. Left panel: cell proliferation was assessed by the MTT reduction assay and the data is shown relative to that of the corresponding untreated controls. Data are the means of multiple independent experiments (N>3). S.D. was less than 10% and thus omitted; **P*<0.05 by one-way ANOVA with Student-Newman-Keuls multiple comparison test. Right panel: the transformants were cultured with or without 5 μg/mL Isa for 24 h. Upper right panel: immunoblot showing the expression of FOXM1 and GAPDH (loading control) in the indicated groups. Lower right panel: reactive oxygen species (ROS) levels were assessed using the ROS assay kit (DOJINDO, Tokyo, Japan) and the data is shown relative to that of the untreated controls. Data are the means ± S.D. (bars) of multiple independent experiments (N=3); *P* values were determined by one-way ANOVA with Student-Newman-Keuls multiple comparison test.

revealed that both Poma and CFZ can induce caspase-dependent apoptosis and trigger ROS production in MM cells.[12,13] In addition, several anti-cancer drugs exert their cytotoxic effects via caspase-dependent degradation of transcriptional regulators like Sp1 or histone deacetylases (HDAC).[14,15] In line with these studies, we found that Poma and CFZ additively enhanced Isa-induced cell death and increased ROS production by promoting downregulation of FOXM1 protein (Figure 2A; *Online Supplementary Figure S1H*). Since treatment with Poma and CFZ, and not Isa, activated caspase-3, caspase-8, and PARP (Figure 2A), we surmise that FOXM1 downregulation may be caused by caspase-dependent degradation. On the other hand, Isa-induced cell death is independent of caspases. Taken together, Poma and CFZ additively enhanced Isa-induced cell death by enhancing FOXM1 downregulation and ROS production.

To identify the downstream targets of FOXM1 *in situ*, we analyzed its binding sites in the genome of KMM.1 cells using chromatin immunoprecipitation with high-throughput DNA sequencing (ChIP-seq). As shown in *Online Supplementary Figure S2A*, over 70% of the peaks corresponding to FOXM1 binding sites located in the vicinity of transcription start sites (TSS). FOXM1 bound to the TSS of genes closely related to MM progression including several genes, such as *NEK2, RGS5*, *UBE2T*, *ANP32E*, and *FAM72A* localized at 1q region. In addition, we found co-occupancy with the H3K27-acetylated regions in the regulatory regions in the 1q+ MM cells but not in the $1q^{normal}$ cells (Figure 2B; *Online Supplementary Figure S2B*). Although all target genes were upregulated in the 1q+ MM cells, the expression levels of *NEK2, UBE2T,* and *FAM72A* showed a significant positive correlation to that of *FOXM1* and the overexpression was significantly associated with worse survival of 1q+ MM patients following TT2/3 (*Online Supplementary Figure S2C*). Likewise, both NEK2 and UBE2T were significantly upregulated in the 1q+ MM cell lines compared to the $1q^{normal}$ cells (Figure 2C). Next, we found that both genetic knockdown and pharmacological inhibition of FOXM1 significantly downregulated NEK2 and UBE2T proteins and mRNA (*Online Supplementary Figure S3A, B*). Furthermore, forced expression of NEK2 and UBE2T significantly mitigated the thiostrepton-induced growth inhibition (*Online Supplementary Figure S3C, D*). These results suggest that NEK2 and UBE2T are the critical downstream targets of FOXM1 in 1q+ MM cells.

We next screened for the global Isa-mediated transcrip-

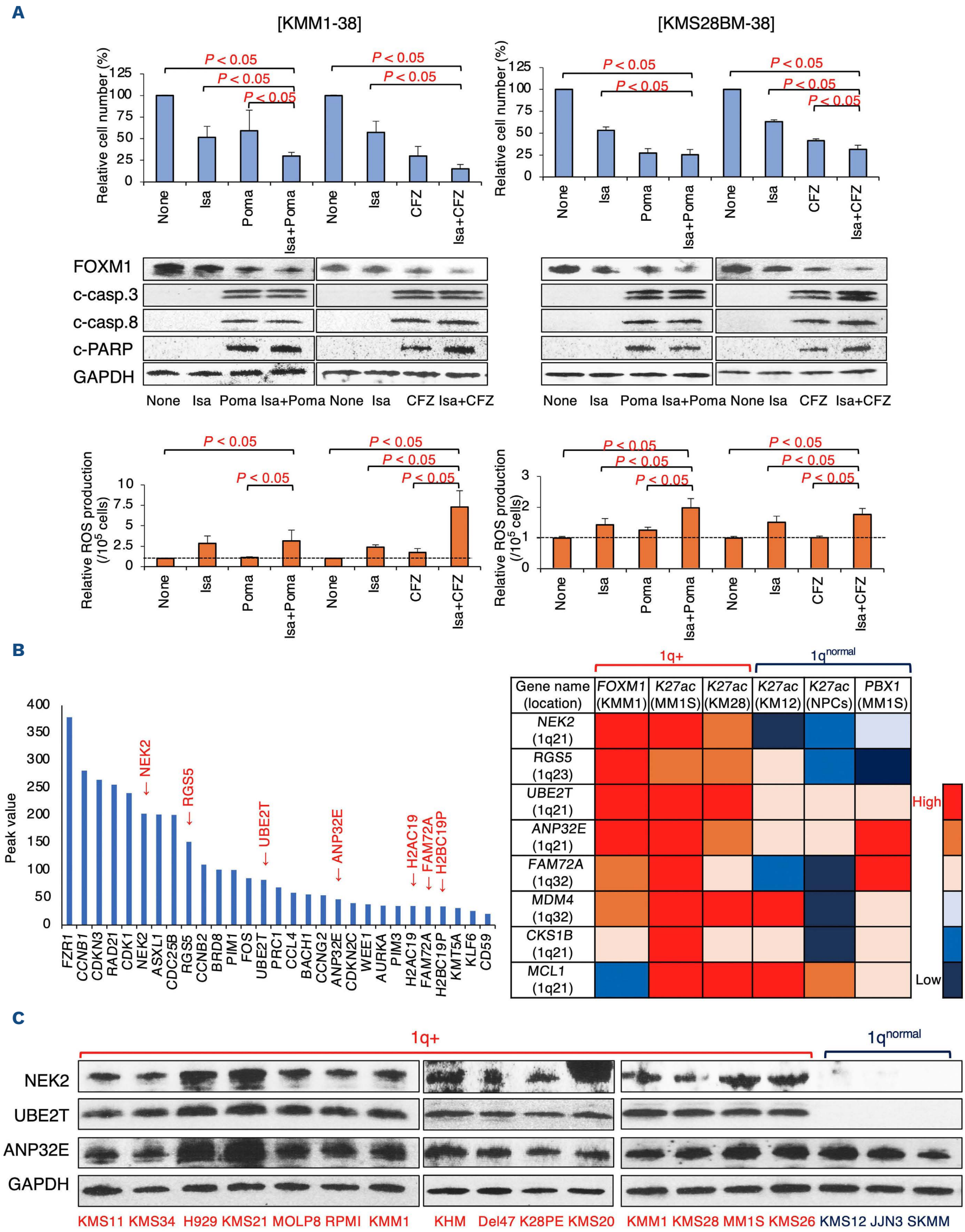

Continued on following page.

Figure 2. Combined effects of isatuximab with pomalidomide or carfilzomib and global analysis of FOXM1 binding in the genome of 1q+ multiple myeloma cells. (A) KMM.1-38 and KMS28BM-38 cells were treated with vehicle (None), 2.5 μg/mL isatuximab (Isa), 2 μM pomalidomide (Poma), 2 nM carfilzomib (CFZ), or their combinations (Isa+Poma or Isa+CFZ) for 24 hours (h). Upper panel: cell proliferation was assessed by the MTT reduction assay and the data is shown relative to that of the corresponding untreated controls (None). Data are the means ± standard deviation (S.D.) (bars) of multiple independent experiments (N=3); *P* values were determined by one-way ANOVA with Student-Newman-Keuls multiple comparison test. Middle panel: immunoblot showing the expression of FOXM1, cleaved caspase-3 (c-casp.3), cleaved caspase-8 (c-casp.8), and cleaved PARP (c-PARP) and GAPDH (loading control) in the indicated groups. Immunoblotting was carried out according to a standard method using the following antibodies: anti-cleaved caspase-3 (#9661), anti-cleaved caspase-8 (#9496), and anti-cleaved PARP (#9541) (Cell Signaling Technology). Lower panel: reactice oxygen species (ROS) levels were assessed using the ROS assay kit and the data is shown relative to that of the corresponding untreated controls (None). Data are the means ± S.D. (bars) of multiple independent experiments (N=3); *P* values were determined by one-way ANOVA with Student-Newman-Keuls multiple comparison test. (B) KMM.1 cells were fixed in 1% formaldehyde at room temperature for 10 minutes (min) and chromatin fractions were isolated by enzymatic shearing. Chromatin immunoprecipitation sequencing (ChIP-seq) was outsourced to Active Motif (Carlsbad, CA, USA), and the data and protocols have been deposited in a MINSEQE-compliant GEO database under accession number GSE279782. We used an antibody against FOXM1 (#20459, CST) validated by Active Motif. Left panel: the peak values of FOXM1 binding sites in the selected genes in KMM.1 cells. Right panel: heat map of the FOXM1/H3K27ac binding at the promoter/enhancer regions of representative genes based on ChIP-seq data. The ChIP-seq data of the following cell types was used: MM.1S (SRX20095564), KMS28BM (SRX7798959), KMS12BM (SRX7798957), and normal plasma cells isolated from healthy volunteers (NPC) (SRX7798977). (C) Immunoblot showing the expression of NEK2, UBE2T, ANP32E, and GAPDH (loading control) in the 1q+ and $1q^{normal}$ MM cell lines. Immunoblotting was carried out according to a standard method using the following antibodies: anti-NEK2 (#14233), anti-UBE2T (#10105) (Proteintech Inc, IL, USA), and anti-ANP32E (#AP20559) (Abcepta, CA, USA).

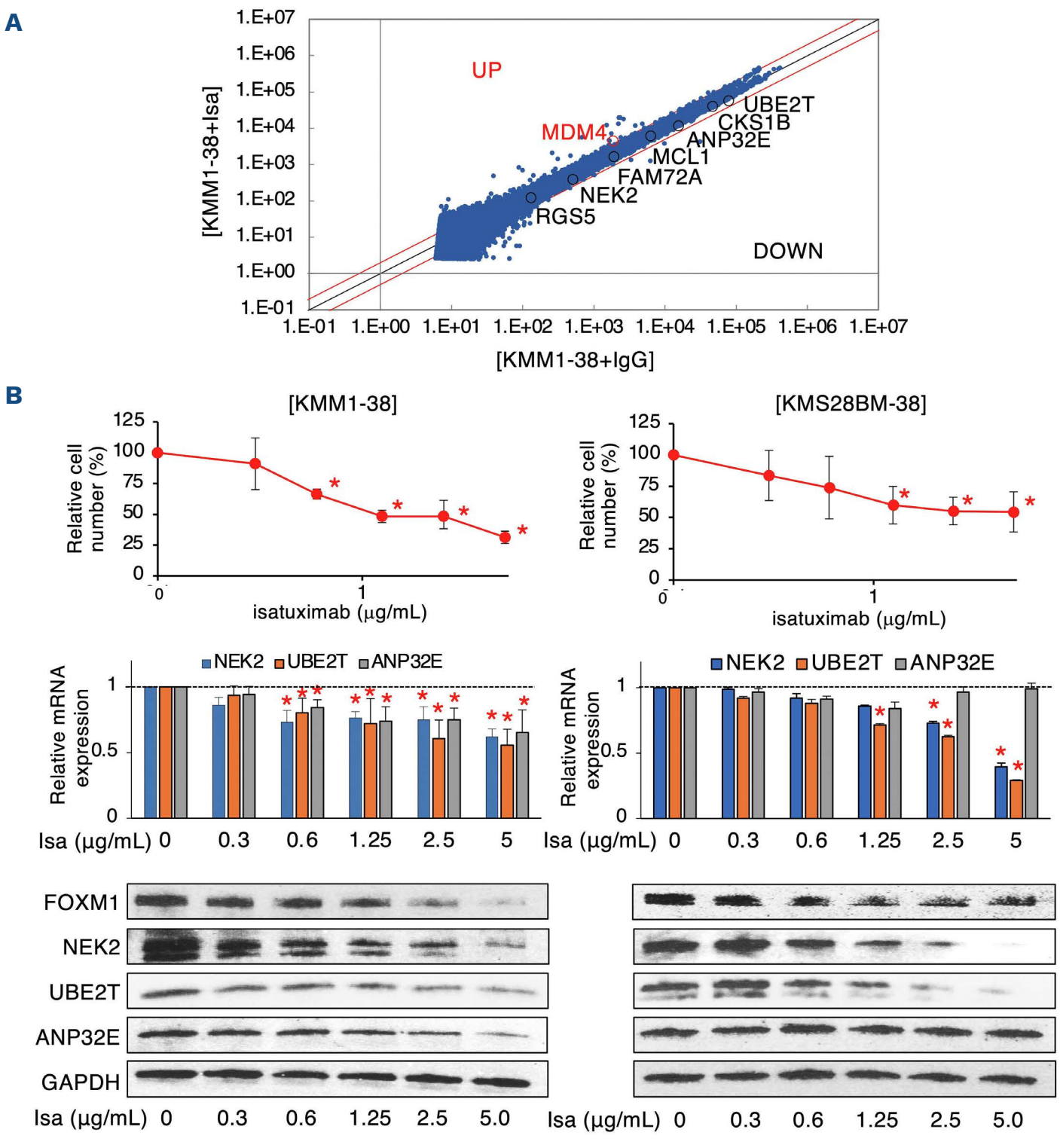

Continued on following page.

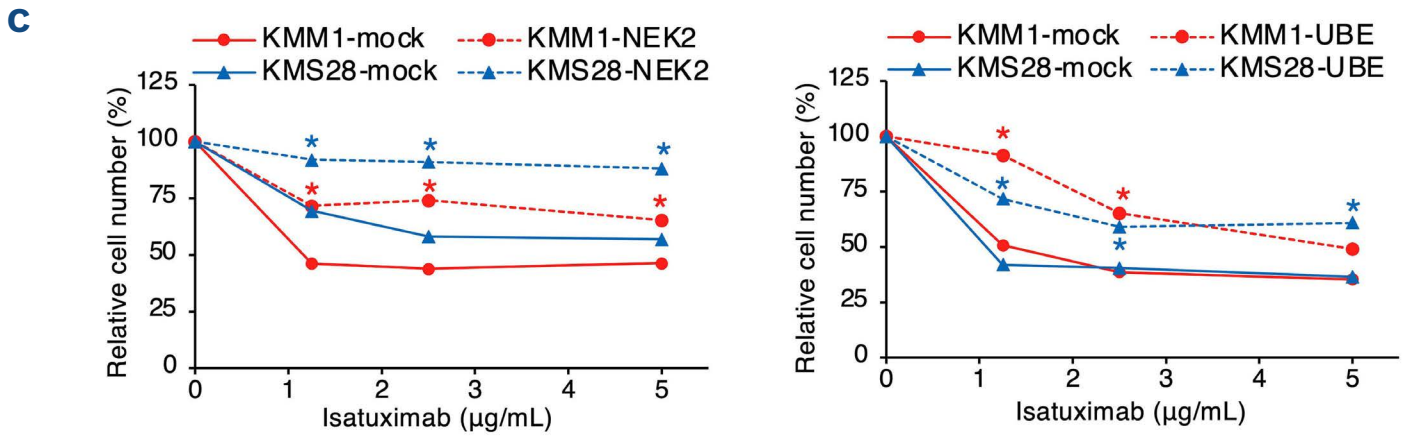

Figure 3. Isatuximab downregulates the expression of NEK2 and UBE2T, both of which were critical downstream targets of FOXM1. (A) KMM.1-38 cells were cultured with 5 μg/mL isatuximab (Isa) (KMM.1-38+Isa) or isotype-matched human immunoglobulin G (hIgG) (KMM.1-38+IgG) for 24 hours (h), and the RNA fractions were isolated. Microarray analysis was performed for 32,078 genes including microRNA. Red lines correspond to 2-fold changes (P<0.05 with a false discovery rate [FDR] threshold of 0.05). Several genes located in chromosome 1q region are annotated. (B) KMM.1-38 and KMS28BM-38 cells were treated with different concentrations of Isa for 24 h. Upper panel: cell proliferation was assessed by the MTT reduction assay and the data is shown relative to that of the corresponding untreated controls. Data are the means ± standard deviation (S.D.) (bars) of multiple independent experiments (N=3). *P<0.05 by one-way ANOVA with Student-Newman-Keuls multiple comparison test. Middle panel: total cellular RNA was isolated from 1-10x10^4 cells using an RNeasy Kit (Qiagen, CA, USA), reverse-transcribed into complementary DNA using ReverTra Ace and oligo(dT) primers (Toyobo, Tokyo, Japan), and subjected to real-time quantitative polymerase chain reaction (QPCR) using the specific primers. The expression levels of candidate FOXM1-target genes (*NEK2*, *UBE2T*, and *ANP32E*) were quantified by the $2^{-\Delta\Delta Ct}$ method using *GAPDH* as the reference and shown as fold changes against untreated control set at 1.0. The means ± S.D. (bars) are of multiple independent experiments (N=3). *P<0.05 by one-way ANOVA with a Student-Newman-Keuls multiple comparison test. We used TaqMan Fast Universal PCR Master Mix and Expression Assays (Hs06629033 for *NEK2*, Hs00928040 for *UBE2T*, Hs05029891 for *ANP32E*, and Hs01922876 for *GAPDH* (Thermo Fisher Scientific, MA, USA). Lower panel: immunoblot showing expression of FOXM1, NEK2, UBE2T, ANP32E, and GAPDH proteins (loading control) in the indicated groups. (C) KMM.1-38 and KMS28BM-38 cells were transduced with either an empty lentiviral vector (mock), NEK2-overexpressing vector (NEK2), or UBE2T-overexpressing vector (UBE) and the stable transformants were treated with different concentrations of Isa for 24 h. We used the lentiviral vector CSII-CMV-MCS-IRES-VENUS containing the coding regions of *NEK2* and *UBE2T* cDNA for gain-of-function experiments. Cell proliferation was assessed by the MTT reduction assay and the data is shown relative to that of the corresponding untreated controls. Data are the means of multiple experiments (N>3); S.D. was less than 10% and thus omitted. *P<0.05 by one-way ANOVA with Student-Newman-Keuls multiple comparison test.

tomic changes in KMM.1-38 cells and found that Isa reduced the expression of several genes including *NEK2* and *UBE2T* (Figure 3A). As anticipated, Isa significantly downregulated NEK2 and UBE2T proteins and mRNA in a dose-dependent manner, which correlated with the cytotoxic effects (Figure 3B). In addition, Isa also downregulated NEK2 and UBE2T in primary MM cells derived from patients with 1q+ (*Online Supplementary Figure S3E*). Consistent with the above findings, overexpression of NEK2 and UBE2T partially mitigated the inhibitory effects of Isa (Figure 3C). These results suggest that Isa induces direct death in 1q+ MM cells via downregulation of the FOXM1/NEK2/UBE2T axis.

In conclusion, we have shown that Isa exerts direct cell death to 1q+ MM cells by downregulating the FOXM1 protein, followed by ROS production and the inactivation of *NEK2* and *UBE2T* genes. Poma and CFZ additively enhanced the cytotoxicity in combination with isatuximab by promoting FOXM1 downregulation and ROS production. However, this study has several limitations. First, we could not obtain sufficient numbers of cells from MM patients to reproduce all data using primary MM cells. Second, we could not confirm that Dara-m and Elo-m are identical to the commercial Dara and Elo. Nevertheless, our findings suggest that Isa exerts direct cell death of 1q+ MM cells by targeting the FOXM1/NEK2/UBE2T axis and provide a rationale for Isa-based therapy for the treatment of 1q+ MM patients from basic standpoints for the first time.

Authors

Jiro Kikuchi,[1] Naoki Osada,[1] Sae Matsuoka,[1] Tomomi Ohta,[2] Hirotaka Kazama,[2] Heigoro Shirai,[2] Marco Meloni,[3] Marielle Chiron,[3] Hiroshi Yasui,[4,5] Hideki Nakasone[1] and Yusuke Furukawa[1,6]

[1]Division of Emerging Medicine for Integrated Therapeutics (EMIT), Center for Molecular Medicine, Jichi Medical University, Shimotsuke, Tochigi, Japan; [2]Sanofi Oncology Medical, Tokyo, Japan; [3]Sanofi R&D, Vitry-sur-Seine, France; [4]Department of Hematology/Oncology, The Institute of Medical Science, University of Tokyo, Tokyo, Japan; [5]Department of Hematology and Oncology, St. Marianna University School of Medicine, Kawasaki, Japan and [6]Center for Medical Education, Teikyo University of Science, Tokyo, Japan

Correspondence:
J. KIKUCHI - kiku-j@jichi.ac.jp
https://doi.org/10.3324/haematol.2025.287904

Received: March 25, 2025.
Accepted: July 21, 2025.
Early view: July 31, 2025.

Disclosures

TO, HK, HS, MM and MC are employees of Sanofi. All other authors have no conflicts of interest to disclose.

Contributions

JK performed experiments, analyzed data, and drafted and finalized the manuscript. NS and SM performed experiments and analyzed data. TO, HK, HS, MM, MC, HY, and HN provided materials and critically reviewed the manuscript; and YF supervised research. All authors read and approved the manuscript before submission.

Acknowledgments

We are grateful to Ms. Mayuka Shiino, Ms. Mai Tadaki, and Ms. Akiko Yonekura for their excellent technical assistance.

Funding

This work was supported by a Sanofi Research Grant (to JK, and YF), Grant-in-Aid for Scientific Research from JSPS, and the Japan Leukemia Research Fund (to JK, NO, and YF), and JK was funded by Takeda Science Foundation, Chugai Foundation for Innovative Drug Discovery Science, Princess Takamatsu Cancer Research Fund, and the International Myeloma Foundation Japan's Grant.

Data-sharing statement

For original data, please contact the corresponding author. ChIP-sequencing data are available at GEO under accession number GSE279782.

References

1. Attal M, Lauwers-Cances V, Hulin C, et al. Lenalidomide, bortezomib, and dexamethasone with transplantation for myeloma. N Engl J Med. 2017;376(14):1311-1320.
2. Facon T, Kumar S, Plesner T, et al. Daratumumab plus lenalidomide and dexamethasone for untreated myeloma. N Engl J Med. 2019;380(22):2104-2115.
3. Pawlyn C, Cairns D, Kaiser M, et al. The relative importance of factors predicting outcome for myeloma patients at different ages: results from 3894 patients in the Myeloma XI trial. Leukemia. 2020;34(2):604-612.
4. Martin T, Richardson PG, Facon T, et al. Primary outcomes by 1q21+ status for isatuximab-treated patients with relapsed/refractory multiple myeloma: subgroup analyses from ICARIA-MM and IKEMA. Haematologica. 2022;107(10):2485-2491.
5. Mohan M, Weinhold N, Schinke C, et al. Daratumumab in high-risk relapsed/refractory multiple myeloma patients: adverse effect of chromosome 1q21 gain/amplification and GEP70 status on outcome. Br J Haematol. 2020;189(1):67-71.
6. Zhu C, Song Z, Wang A, et al. Isatuximab acts through Fc-dependent, independent, and direct pathways to kill multiple myeloma cells. Front Immunol. 2020;11:1771.
7. Trasanidis N, Katsarou A, Ponnusamy K, et al. Systems medicine dissection of chr1q-amp reveals a novel PBX1-FOXM1 axis for targeted therapy in multiple myeloma. Blood. 2022;139(13):1939-1953.
8. Ivanov A, Beers SA, Walshe CA, et al. Monoclonal antibodies directed to CD20 and HLA-DR can elicit homotypic adhesion followed by lysosome-mediated cell death in human lymphoma and leukemia cells. J Clin Invest. 2009;119(8):2143-5219.
9. Honeychurch J, Alduaij W, Azizyan M, et al. Antibody-induced nonapoptotic cell death in human lymphoma and leukemia cells is mediated through a novel reactive oxygen species-dependent pathway. Blood. 2012;119(15):3523-3533.
10. Su G, Yang Q, Zhou H, et al. Thiostrepton as a potential therapeutic agent for hepatocellular carcinoma. Int J Mol Sci. 2024;25(17):9717.
11. Okuni N, Honma Y, Urano T, Tamura K. Romidepsin and tamoxifen cooperatively induce senescence of pancreatic cancer cells through downregulation of FOXM1 expression and induction of reactive oxygen species/lipid peroxidation. Mol Biol Rep. 2022;49(5):3519-3529.
12. Sebastian S, Zhu YX, Braggio E, et al. Multiple myeloma cells' capacity to decompose H2O2 determines lenalidomide sensitivity. Blood. 2017;129(8):991-1007.
13. Fink EE, Mannava S, Bagati A, et al. Mitochondrial thioredoxin reductase regulates major cytotoxicity pathways of proteasome inhibitors in multiple myeloma cells. Leukemia. 2016;30(1):104-111.
14. Kikuchi J, Wada T, Shimizu R, et al. Histone deacetylases are critical targets of bortezomib-induced cytotoxicity in multiple myeloma. Blood. 2010;116(3):406-417.
15. Hiraoka N, Kikuchi J, Koyama D, et al. Alkylating agents induce histone H3K18 hyperacetylation and potentiate HDAC inhibitor-mediated global histone acetylation and cytotoxicity in mantle cell lymphoma. Blood Cancer J. 2013;3(12):e169.